Article:
Zhu, Z.Q., Xia, Z.P., Shi, Y.F. et al. (2003) Performance of Halbach magnetized brushless AC motors. IEEE Transactions on Magnetics, 39 (5 (Par). pp. 2992-2994. ISSN: 0018-9464

https://doi.org/10.1109/TMAG.2003.816717

Performance of Halbach Magnetized Brushless AC Motors

Z. Q. Zhu, *Senior Member, IEEE*, Z. P. Xia, Y. F. Shi, D. Howe, A. Pride, and X. J. Chen

***Abstract*—The steady-state performance of Halbach magnetized brushless ac machines when operated in constant torque and flux-weakening modes is investigated both theoretically and experimentally, with particular emphasis on the influence of cross-coupling magnetic saturation on the torque capability.**

***Index Terms*—Brushless machines, permanent magnet machines, permanent magnets, torque control.**

I. Introduction

HALBACH magnetized brushless machines exhibit an essentially sinusoidal airgap field distribution and a sinusoidal back-emf waveform, as well as negligible cogging torque, without employing skew or a distributed winding. Thus, they are eminently suitable for brushless ac operation. While Halbach machines often employ segmented magnets to realize an approximate Halbach magnetization [1], [2], in this paper an anisotropic bonded NdFeB Halbach magnetized ring magnet is employed. The magnet is produced by orienting the NdFeB injection moulding compound in a powder alignment system [3], and subsequently impulse magnetizing it in a Halbach field. The features of such a Halbach magnetized machine, in terms of its airgap field distribution and back-emf and cogging torque waveforms, have been compared with those which result with a Halbach magnet fabricated from discrete magnet segments [2]. However, the control performance of Halbach magnetized machines has not been reported. Thus, this paper investigates the steady-state performance of a Halbach magnetized brushless ac machine in constant torque and flux-weakening modes, both theoretical and experimentally. It also investigates the influence of cross-coupling magnetic saturation on the torque capability.

II. Main Features of Motor and Torque/Flux-Weakening Control

A Halbach magnetized machine is a form of surface-mounted magnet machine. The prototype motor is supplied from a dc link voltage of 21 V, its rated peak phase current being 45 A. The stator has 18 slots, which accommodate a three-phase nonoverlapping winding, while the rotor has no back-iron and is equipped with a 12-pole anisotropic bonded NdFeB Halbach magnetized magnet, as shown in Fig. 1(a). In the constant torque mode below base-speed, maximum torque per ampere control is used, which results in zero d-axis current since the rotor does not exhibit saliency. Above base-speed, when the motor operates under both supply voltage and current limitations, flux-weakening control is employed to maximize the power [4], [5]. Maximum flux-weakening performance is achieved [6] by designing the machine such that $\psi_m = L_d I_a$, where I_a is the rated phase current, L_d is the d-axis inductance and ψ_m is the stator winding flux-linkage produced by the rotor magnet.

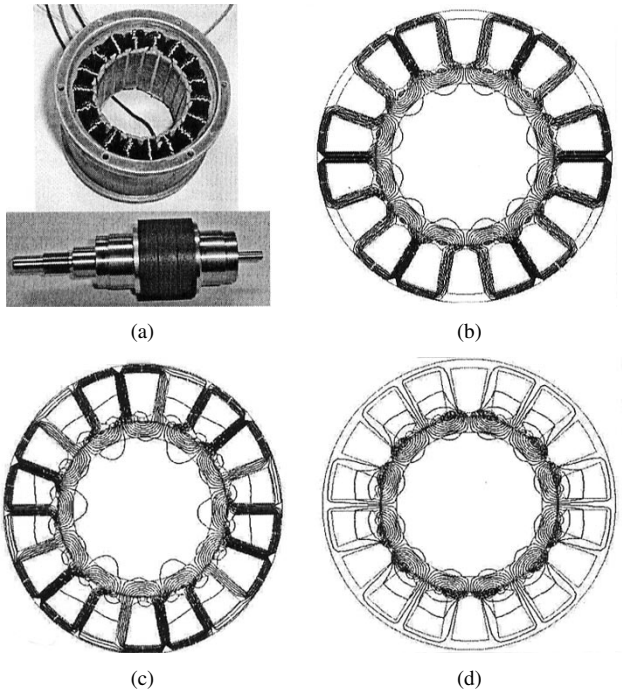

Fig. 1. Prototype Halbach magnetized brushless ac motor and typical field distributions: (a) stator and rotor, (b) open circuit, (c) rated current ($I_d = 0,\ I_q = 45$ A), and (d) rated current ($I_d = 45$ A, $I_q = 0$).

Due to their relatively low winding inductance and demagnetization withstand capability, surface-mounted magnet brushless motors are generally perceived as having a limited flux-weakening capability. However, although the Halbach magnetized machine is also a surface-mounted magnet motor topology, it has been designed to have 1.0 per-unit winding inductance by appropriately designing the stator teeth and slot openings so that the majority of the d-axis armature reaction flux does not pass through the magnets but instead passes across the stator slot openings. Hence, a high level of flux-weakening and demagnetization withstand capability can be achieved, as will be demonstrated later.

Manuscript received January 8, 2003.

Z. Q. Zhu, Z. P. Xia, Y. F. Shi, and D. Howe are with the Department of Electronic and Electrical Engineering, University of Sheffield, Sheffield S1 3JD, U.K. (e-mail: Z.Q.Zhu@sheffield.ac.uk; z.p.xia@sheffield.ac.uk; ELP00YS@sheffield.ac.uk; D.Howe@sheffield.ac.uk).

A. Pride and X. J. Chen are with IMRA Europe S.A., U.K. Research Centre, University of Sussex, Brighton BN1 9RS, U.K. (e-mail: AP@imra-ukrc.com; XC@imra-ukrc.com).

Digital Object Identifier 10.1109/TMAG.2003.816717

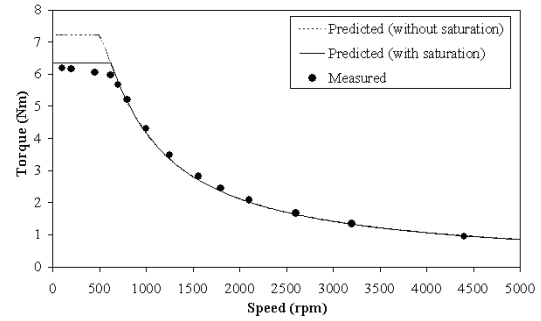

(a)

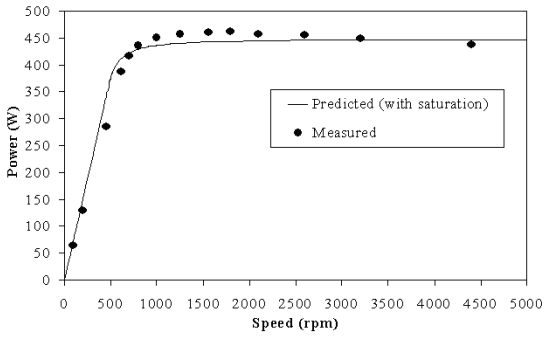

(b)

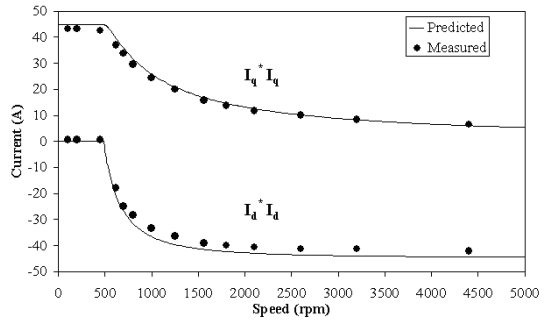

(c)

Fig. 2. Comparison of predicted and measured torque/power/current-speed characteristics ($I_a = 45$ A): (a) torque, (b) power, and (c) d- and q-axis current.

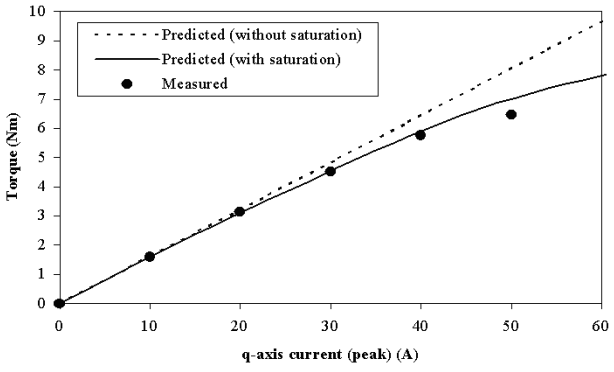

Fig. 3. Influence of saturation on torque capability at 200 r/min.

III. Finite–Element Calculations and Experimental Validation

Fig. 1(b)–(d) shows field distributions when the Halbach magnetized machine is on open-circuit and carries rated current

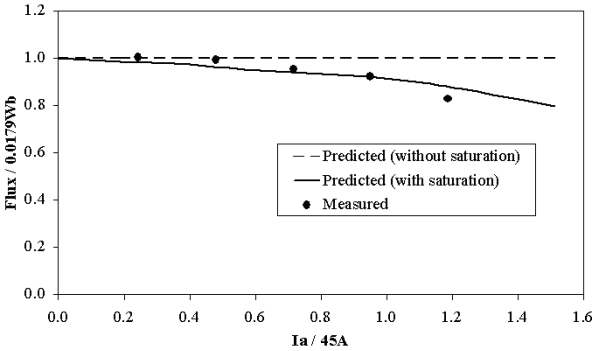

Fig. 4. Variation ofψ_m with phase current at 200 r/min.

($I_d = 0$, $I_q = 45$ A and $I_d = -45$ A, $I_q = 0$), while Fig. 2 compares analytically predicted and measured torque, power, and d axis and q axis current versus speed characteristics. The predicted characteristics are obtained from the steady-state equations given in [4]. Finite-element calculated parameters, such as ψ_m, L_d, and L_q, are used in the predictions, as well as in the DSP-implemented control strategy, with due account for magnetic saturation. Good agreement is achieved, as shown in Figs. 4—6. For comparison, the predicted torque using the unsaturated value of flux linkage $\psi_m = \psi_{\max} = 0.0179$ Wb and unsaturated d- and q-axis inductances $L_d = L_q = 0.4$ mH are also shown in Figs. 2(a) and 3. It can be seen that the measured torque in the constant torque mode (i.e., below the base-speed of $\sim$860 r/min) is significantly lower than the predicted value when saturation is neglected. This is due to the effect of cross-coupling saturation between the magnetic field produced by the Halbach magnetized magnet and that produced by the q-axis armature reaction field. This causes ψ_m, and consequently the torque, to reduce significantly as the q-axis current increases, as shown in Figs. 3 and 4, in which the predicted torque is calculated by Maxwell stress integration, while the magnet flux-linkage is calculated from

$$\psi_m = \frac{T}{(3/2)pI_q}$$

where T is either predicted or measured (in Newton meters), p is the number of pole-pairs, andI_q is the q-axis component of the stator current.

From Fig. 2(a), it can be seen that the influence of cross-coupling saturation is significant only at low speed, i.e., in the constant torque range. In the high-speed range, i.e., flux-weakening mode, the demagnetizing current I_d is increased progressively while I_q is correspondingly reduced so that the resultant phase current is maintained at the rated value. Consequently, the cross-coupling effect gradually diminishes. For simplicity, it can be assumed that ψ_m depends on the speed, having a minimum saturated value below base speed and a maximum unsaturated value above base speed. A simple curve fit is employed to represent the variation of ψ_m from the saturated condition to the unsaturated condition, as shown in Fig. 5, when maximum torque per ampere control is employed.

Due to the cross coupling, the d- and q-axis inductances, L_d and L_q, are usually coupled to some extent. However, for sim-

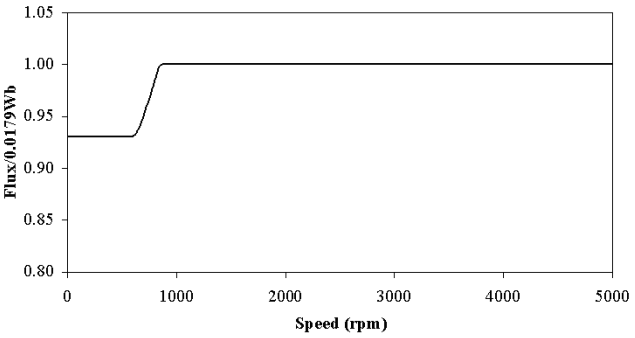

Fig. 5. Curve fit to predicted variation of ψ_m with speed.

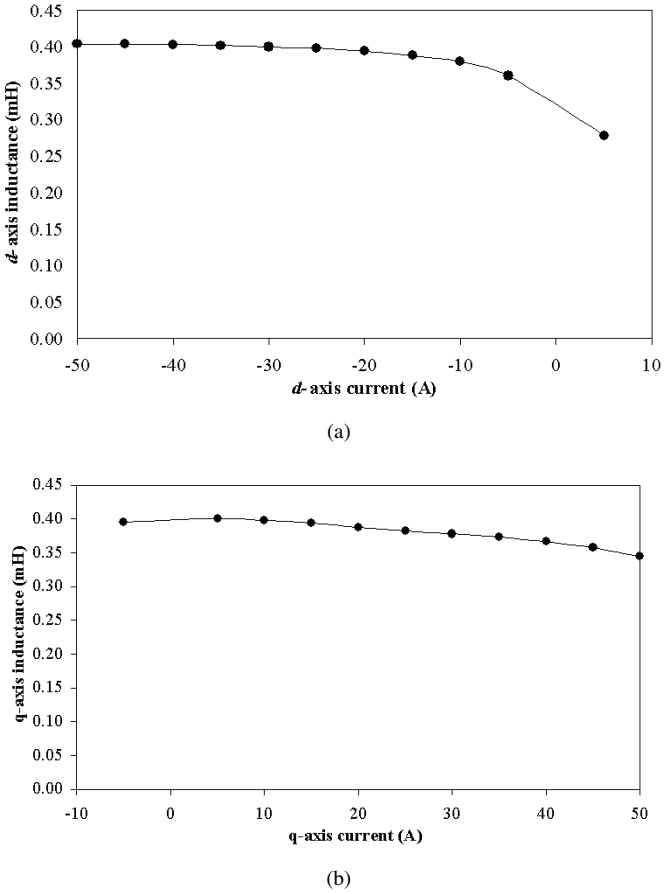

Fig. 6. Variation of finite element predicted inductances with current: (a) d-axis inductance and (b) q-axis inductance.

plicity, they have been assumed to be decoupled, i.e., L_d depends only on I_d and L_q depends only on I_q, as shown in Fig. 6. Similar to its influence on ψ_m, the demagnetizing current I_d causes the magnetic circuit to gradually become less saturated above base speed. Consequently, L_d increases initially before becoming almost constant, as the magnetic circuit becomes effectively linear at a sufficiently high demagnetizing current, viz. $I_d < -20$ A. In regards to L_q, it is almost constant when $I_q < 15$ A, and then gradually reduces as the cross coupling between the magnet flux and the q-axis flux increases. However, as shown in Fig. 6, the influence of magnetic saturation on the d- and q-axis inductances is relatively small for the prototype motor due to its relatively large effective airgap, since it has no rotor back-iron. In addition, the variation of L_d and L_q does not affect the torque–speed characteristic in the constant torque range, since $I_d = 0$ control is employed, and the torque is determined by

$$T = (3/2)p\psi_m I_q.$$

However, in the flux-weakening range, while the variation of L_d and L_q influences the d- and q-axis current components, particularly at high speed, it does not significantly influence the torque–speed characteristic since the rotor is nonsalient.

Overall, the influence of the reduction in ψ_m due to the influence of cross-coupling magnetic saturation, on the torque capability in the constant torque range, is much more significant than that of the d- and q-axis inductances.

IV. Conclusion

The steady-state performance of a Halbach magnetized brushless ac machine when operating in the constant torque and flux-weakening modes has been investigated both theoretically and experimentally. It has been shown that the torque capability in the constant torque range is influenced significantly by magnetic saturation due to the effect of cross coupling between the magnetic field produced by the Halbach magnetized magnet and the q-axis armature reaction field. This causes the stator flux-linkage ψ_m and, consequently, the torque to reduce as the q-axis current increases. It has also been shown that the influence of the cross coupling on ψ_m is much more significant than that on the d- and q-axis inductances in terms of compromising the achievable torque.

References

[1] K. Halbach, "Design of permanent magnet multipole magnets with oriented rare earth cobalt material," *Nucl. Instrum. Methods*, vol. 169, pp. 1–10, 1980.

[2] Z. Q. Zhu, Z. P. Xia, and D. Howe, "Comparison of Halbach magnetized brushless machines having discrete magnet segments or single ring magnet," *IEEE Trans. Magn.*, vol. 38, pp. 2997–2999, 2002.

[3] Z. Q. Zhu, Z. P. Xia, K. Atallah, G. W. Jewell, and D. Howe, "Powder alignment system for anisotropic bonded NdFeB Halbach cylinders," *IEEE Trans. Magn.*, vol. 36, pp. 3349–3352, 2000.

[4] S. Morimoto, M. Sanada, and Y. Takeda, "Wide-speed operation of interior permanent magnet synchronous motors with high-performance current regulator," *IEEE Trans. Indust. Applicat.*, vol. 30, pp. 920–926, 1994.

[5] T. M. Jahns, "Flux-weakening regime operation of an interior permanent magnet synchronous motor drive," *IEEE Trans. Indust. Applicat.*, vol. 23, pp. 681–689, 1987.

[6] W. L. Soong and T. J. E. Miller, "Field-weakening performance of brushless synchronous ac motor drives," in *IEE Proc.-Electr. Power Applicat.*, vol. 141, 1994, pp. 331–340.